Energy-Aware UAV-Enabled Target Tracking: Online Optimization with Location Constraints

Yifan Jiang, Qingqing Wu, *Senior Member, IEEE*, Wen Chen, *Senior Member, IEEE*, Hongxun Hui, *Member, IEEE*

***Abstract*—Energy-aware unmanned aerial vehicle (UAV) trajectory design has been a crucial issue to address in UAV-assisted wireless networks. However, unlike traditional offline designs, online UAV trajectory designs in target tracking scenarios are non-trivial in concurrently satisfying the total propulsion energy consumption constraint and the initial-final location constraint due to the undetermined information. To address this issue, we propose a novel online UAV trajectory optimization approach for the weighted sum-predicted posterior Cramér-Rao bound (PCRB) minimization, which guarantees the feasibility of satisfying the two mentioned constraints. Specifically, our proposed approach designs the UAV trajectory by solving two subproblems: the candidate trajectory optimization problem and the energy-aware backup trajectory optimization problem. Then, we propose an algorithm converging to the global optimal solution to the candidate trajectory optimization problem based on Dinkelbach's transform and the Lasserre hierarchy. The energy-aware backup trajectory optimization problem is efficiently solved by the successive convex approximation method. Numerical results illustrate the effectiveness of our proposed approach and its significant superiority to the existing approach and benchmark regarding sensing performance and energy utilization flexibility.**

***Index Terms*—UAV trajectory, propulsion energy, online tracking**

I. Introduction

The emerging applications of unmanned aerial vehicles (UAVs) in next-generation wireless networks have recently received substantial research interest, including UAV-enabled integrated communication and sensing (ISAC) [1]–[3]. The advantages of UAVs are mainly threefold: favorable channel conditions due to the high line-of-sight (LoS) probability, flexible deployment due to the high mobility with low cost, and additional system design degrees of freedom (DoFs) due to the controllable UAV trajectory [3]. Therefore, substantial existing works investigated UAV trajectory optimization for performance maximization of UAV-assisted wireless systems. For example, the throughput of a UAV relay was maximized in [4] via joint power allocation and trajectory optimization. In [5], the minimum throughput of a multi-UAV multi-user communication network was maximized by jointly optimizing the user association, UAV's transmit power, and trajectory. For practical UAV trajectory design, energy consumption and efficiency gradually become important factors to consider due to the limited onboard energy [6]–[9], which is different from conventional airborne radars. For instance, UAV trajectory optimization algorithms to maximize the energy efficiency and to minimize the energy consumption were proposed in [6] and [7] for fixed-wing and rotary-wing UAVs, respectively. In [8], an efficient UAV trajectory planning algorithm was proposed to minimize the propulsion energy consumption of a cellular-connected UAV acting as a synthetic aperture radar. Additionally, joint resource allocation and UAV trajectory optimization were studied in [9] to minimize the total energy consumption of a single-UAV ISAC system. However, most existing works, like [4]–[9], have focused on offline UAV trajectory designs, which are inapplicable in real-time target tracking scenarios.

To solve this issue, a few recent works come up with online UAV trajectory designs for target tracking subject to the total energy consumption constraint [10], [11]. Specifically, a multi-stage UAV trajectory optimization approach was proposed in [10] to maximize a unified ISAC performance bound. In [11], a slot-by-slot UAV trajectory optimization approach was proposed to minimize the predicted posterior Cramér-Rao bound (PCRB) for the estimated target motion state. Both approaches were based on the successive convex approximation (SCA) technique, which only guarantees convergence to a locally optimal solution. Meanwhile, both works ignored the initial-final location constraint, which practically models scenarios like launching and landing in predetermined locations.

Motivated by the above issues, we study the online UAV trajectory design in a UAV-enabled target tracking system with location constraints, where a UAV tracks a moving target via the classic extended Kalman filtering (EKF) method during its flight from the initial location to the final location. Specifically, the UAV trajectory within a short period is optimized to minimize the weighted sum of predicted PCRBs for state estimation. The main contributions of this work are summarized as follows: **1)** We propose a novel UAV trajectory optimization approach, which solves two subproblems to optimize a candidate UAV trajectory for the weighted sum-predicted PCRB minimization and a backup UAV trajectory for the propulsion energy minimization, respectively. Our proposed approach achieves flexible energy utilization for sensing performance maximization and ensures the feasibility of the optimized UAV trajectory. **2)** We propose an algorithm that optimally solves the weighted sum-predicted PCRB minimization

This work is funded in part by Guangdong science and technology program under grant 2022A0505050011 and in part by the Science and Technology Development Fund, Macau SAR (File no. 001/2024/SKL, File no. 0117/2022/A3).

Yifan Jiang is with the State Key Laboratory of Internet of Things for Smart City, University of Macau, Macao 999078, China (email: yc27495@umac.mo) and also with Shanghai Jiao Tong University, Shanghai 200240, China. Qingqing Wu and Wen Chen are with the Department of Electronic Engineering, Shanghai Jiao Tong University, Shanghai 200240, China (e-mail: {qingqingwu@sjtu.edu.cn; wenchen@sjtu.edu.cn}). Hongxun Hui is with the State Key Laboratory of Internet of Things for Smart City and Department of Electrical and Computer Engineering, University of Macau, Macao, 999078 China (email: hongxunhui@um.edu.mo).

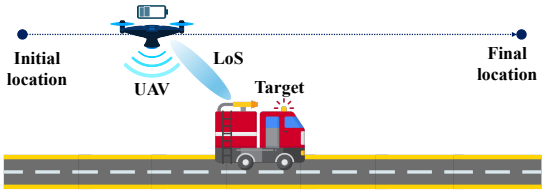

Fig. 1. A UAV-enabled target tracking system with location constraints.

problem based on Dinkelbach's transform with the Lasserre hierarchy. The backup UAV trajectory optimization problem is efficiently solved by another proposed algorithm based on the successive convex approximation (SCA) method. **3)** Simulation results validate our proposed approach's effectiveness and show its superiority to the existing SCA algorithm in optimality and significant sensing performance improvement with more flexible energy utilization over the benchmark.

II. System Model and Problem Formulation

As shown in Fig.1, we consider a UAV-enabled target tracking system, where a UAV is dispatched from the initial location $x_{\rm I}$ to the final location $x_{\rm F}$ within a predetermined flight duration T in order to track a moving ground target. To be specific, it is assumed that both the UAV and the target motion state, i.e., their position and velocity, remain constant during a short period ΔT [9]. As such, by discretizing the whole flight duration T into $N = T/\Delta T$ time slots, the relative motion state of the target with respect to the UAV can be expressed as $\mathbf{x}_n = [x_n, v_n]^T$, where x_n and v_n denotes the relative position and velocity, respectively. As an initial work, it is assumed that both the UAV and the target follow the one-dimensional horizontal movement. In addition, the UAV flies at a fixed altitude H and is equipped with a uniform linear array (ULA) with $N_{\rm t}$ transmit antennas and a ULA with $N_{\rm r}$ receive antennas parallel to the horizontal path.[1]

A. Signal and Measurement Model

Let $s_n(t) \in \mathbb{C}$ denote the equivalent baseband signal transmitted with the power $P_{\rm A}$ at the nth time slot. In this work, we assume that the air-to-ground channel can be modeled as a single LoS path with free space path loss, thanks to the scarce blockage in the vertical dimension and the UAV maneuverability, especially in rural areas [3]. Moreover, the target radar cross section (RCS) remains approximately constant among different time slots [9], and the negative impacts of clutter can be suppressed [1]. Then, the large-scale sensing channel gain can be represented by $G_n = \beta_{\rm r} d_n^{-4}$ with $\beta_{\rm r} = \lambda^2\varepsilon/(64\pi^3)$, where λ denotes the carrier wavelength, ε denotes the target RCS and d_n denotes the distance from the target to the UAV at the nth time slot. Next, the sensing channel can be expressed as $\mathbf{h}_n = \sqrt{G_n} e^{-j4\pi\frac{d_n}{\lambda}} \mathbf{b}(\phi_n)\mathbf{a}^H(\phi_n)$, where $\mathbf{a}(\phi) = [e^{j\frac{\pi(N_{\rm t}-1)\cos\phi}{2}}, ..., e^{-j\frac{\pi(N_{\rm t}-1)\cos\phi}{2}}]^T$ and $\mathbf{b}(\phi) = [e^{j\frac{\pi(N_{\rm r}-1)\cos\phi}{2}}, ..., e^{-j\frac{\pi(N_{\rm r}-1)\cos\phi}{2}}]^T$ denote the UAV transmit and receive array response vectors, respectively, and ϕ_n denotes the elevation angle of the geographical path connecting the UAV to the target at the nth time slot. The echo signals can be represented by $\mathbf{r}_n(t) = \sqrt{P_{\rm A}}\mathbf{h}_n e^{j2\pi\mu_n t}\mathbf{f}_n s_n(t-\tau_n) + \mathbf{z}_{{\rm r},n}(t)$, where μ_n denotes the Doppler shift, $\mathbf{f}_n$ denotes the transmit beamforming vector, τ_n denotes the round-trip time delay, and $\mathbf{z}_{{\rm r},n}(t) \in \mathbb{C}^{N_{\rm r}\times 1}$ denotes the complex additive white Gaussian noise with zero mean and variance of σ^2.

At the nth time slot, the elevation angle, the distance, and the Doppler shift can be measured via the maximum likelihood estimation and the matched filtering, respectively [12]. To be specific, the measured results can be given by $\hat{\phi}_n = \phi_n + z_{1,n}$, $\hat{d}_n = d_n + z_{2,n}$ and $\hat{\mu}_n = \mu_n + z_{3,n}$, where $z_{i,n} \sim \mathcal{N}\left(0, \sigma_{i,n}^2\right), i = 1,2,3$ denotes the measurement noise. The measurement noise variances $\sigma_{i,n}^2, i = 1,2,3$ are modelled as $\sigma_{1,n}^2 = a_1^2/\gamma_n \sin^2\phi_n$ and $\sigma_{i,n}^2 = a_i^2/\gamma_n, i = 2,3$, respectively, where a_i denotes the coefficients based on system configuration, $\gamma_n = \gamma_{\rm r}/d_n^2$ denotes the sensing signal-to-noise ratio, and $\gamma_{\rm r}$ is defined as $\gamma_{\rm r} \triangleq N_{\rm t}N_{\rm r}P_{\rm A}N_{\rm sym}\beta_{\rm r}/\sigma^2$ with $N_{\rm sym}$ denoting the matched filtering gain [12].

B. Target Tracking Model

We assume that the target movement follows the classic constant-velocity model [13]. In particular, the relative motion state at the nth time slot is evolved from the counterpart at the $(n-1)$th time slot as $\mathbf{x}_n = \mathbf{G}\mathbf{x}_{n-1} - \mathbf{u}_{{\rm A},n} + \mathbf{z}_{{\rm p},n}$, where $\mathbf{G}$ denotes the transition matrix, $\mathbf{u}_{{\rm A},n} = [(v_{{\rm A},n} - v_{{\rm A},n-1})\Delta T, (v_{{\rm A},n} - v_{{\rm A},n-1})]^T$ denotes the UAV motion state increment at the nth time slot, $v_{{\rm A},n}$ denotes the UAV velocity at the nth time slot, and $\mathbf{z}_{{\rm p},n} \sim \mathcal{N}(\mathbf{0}, \mathbf{Q}_{\rm p})$ denotes the Gaussian process noise with zero mean and the covariance matrix $\mathbf{Q}_{\rm p}$. According to the constant-velocity model, the expressions of $\mathbf{G}$ and $\mathbf{Q}_{\rm p}$ can be specified as

$$\mathbf{G} = \begin{bmatrix} 1 & \Delta T \\ 0 & 1 \end{bmatrix}, \mathbf{Q}_s = \begin{bmatrix} \frac{1}{3}\Delta T^3 & \frac{1}{2}\Delta T^2 \\ \frac{1}{2}\Delta T^2 & \Delta T \end{bmatrix} \tilde{q}, \tag{1}$$

respectively, where $\tilde{q}$ denotes the process noise intensity [13].[2]

To track the target with time-varying motion state, online relative motion state estimation is performed based on the EKF method [12].[3] Under the EKF framework, the predicted state variables $\breve{\mathbf{x}}_n = [\breve{x}_n, \breve{v}_n]^T$ can be obtained as

$$\breve{\mathbf{x}}_n = \mathbf{G}\hat{\mathbf{x}}_{n-1} - \mathbf{u}_{{\rm A},n}, \tag{2}$$

where $\hat{\mathbf{x}}_{n-1}$ denotes the estimated state variables at the $(n-1)$th time slot. Then, the measured results $\mathbf{y}_n \triangleq [\hat{\phi}_n, \hat{\tau}_n, \hat{\mu}_n]^T$ can be compactly expressed as $\mathbf{y}_n = \mathbf{h}(\mathbf{x}_n) + \mathbf{z}_{{\rm m},n}$, where the function $\mathbf{h}(\cdot)$ can be obtained from $\phi_n = \arctan(\frac{H}{x_n})$, $d_n = \sqrt{H^2 + x_n^2}$ and $\mu_n = -\frac{2v_n x_n}{\lambda\sqrt{x_n^2+H^2}}$, and $\mathbf{z}_{{\rm m},n} = [z_{1,n}, z_{2,n}, z_{3,n}]^T \sim \mathcal{N}(\mathbf{0}, \mathbf{Q}_{{\rm m},n})$ denotes the measurement noise vector with the covariance matrix denoted by $\mathbf{Q}_{{\rm m},n} = {\rm diag}(\sigma_{1,n}^2, \sigma_{2,n}^2, \sigma_{3,n}^2)$. Next, the state prediction mean square error (MSE) matrix $\mathbf{M}_{{\rm p},n}$ and the Kalman gain matrix $\mathbf{K}_n$ can calculated by $\mathbf{M}_{{\rm p},n} = \mathbf{G}\mathbf{M}_{n-1}\mathbf{G}^H + \mathbf{Q}_{\rm p}$ and $\mathbf{K}_n = \mathbf{M}_{{\rm p},n}\mathbf{H}_n^H(\mathbf{Q}_{{\rm m},n} + \mathbf{H}_n\mathbf{M}_{{\rm p},n}\mathbf{H}_n^H)^{-1}$, respectively, where $\mathbf{M}_{n-1}$

[1]Our proposed approach can be readily extended to the case with three-dimensional UAV movement by considering the UAV velocity as a vector and expanding the dimension of state variable vector $\mathbf{x}_n$.

[2]The expressions of $\mathbf{G}$ and $\mathbf{Q}_{\rm p}$ can be derived from the discretion of the continuous-time state equation given by the constant-velocity model [13], in which the process noise models the random slight disturbance of target velocity in practice.

[3]In our work, the measurement model is non-linear with respect to $\mathbf{x}_n$, therefore necessitating EKF instead of the classic linear Kalman filtering to track the target.

$$F_{\mathrm{x}}(\breve{\mathbf{x}}_n)=\frac{H^4\gamma_{\mathrm{r}}}{a_1^2(H^2+\breve{x}_n^2)^5}+\frac{\gamma_{\mathrm{r}}\breve{x}_n^2}{a_2^2(H^2+\breve{x}_n^2)^3}+\frac{4H^4\gamma_{\mathrm{r}}\breve{v}_n^2}{a_3^2\lambda^2(H^2+\breve{x}_n^2)^5}+r_{n,11},\quad F_{\mathrm{v}}(\breve{\mathbf{x}}_n)=\frac{4\gamma_{\mathrm{r}}\breve{x}_n^2}{a_3^2\lambda^2(H^2+\breve{x}_n^2)^3}+r_{n,22}, \tag{4}$$

$$D(\breve{\mathbf{x}}_n)=F_{\mathrm{x}}(\breve{\mathbf{x}}_n)F_{\mathrm{v}}(\breve{\mathbf{x}}_n)-\left(r_{n,12}+\frac{4H^2\gamma_{\mathrm{r}}\breve{v}_n\breve{x}_n}{a_3^2\lambda^2(H^2+\breve{x}_n^2)^4}\right)\left(r_{n,21}+\frac{4H^2\gamma_{\mathrm{r}}\breve{v}_n\breve{x}_n}{a_3^2\lambda^2(H^2+\breve{x}_n^2)^4}\right),\quad r_{n,ij}=[\mathbf{M}_{\mathrm{p},n}^{-1}]_{ij}, \tag{5}$$

$$P(v_{\mathrm{A},n})=P_0\left(1+3v_{\mathrm{A},n}^2/U_{\mathrm{tip}}^2\right)+P_{\mathrm{i}}\left(\left(1+v_{\mathrm{A},n}^4/4v_{\mathrm{h}}^4\right)^{1/2}-v_{\mathrm{A},n}^2/2v_{\mathrm{h}}^2\right)^{1/2}+\frac{1}{2}\chi|v_{\mathrm{A},n}|^3, \tag{6}$$

denotes the estimation MSE matrix at the $(n-1)$th time slot and $\mathbf{H}_n$ denotes the Jacobian matrix for $\mathbf{h}(\cdot)$ with respect to the predicted state variables specified as

$$\mathbf{H}_n=\left.\frac{\partial\mathbf{h}}{\partial\mathbf{x}_n}\right|_{\mathbf{x}_n=\breve{\mathbf{x}}_n}=\begin{bmatrix}\frac{-H}{H^2+\breve{x}_n^2} & \frac{\breve{x}_n}{\sqrt{H^2+\breve{x}_n^2}} & \frac{-2\breve{v}_nH^2}{\lambda\sqrt{(H^2+\breve{x}_n^2)^3}}\\ 0 & 0 & \frac{-2\breve{x}_n}{\lambda\sqrt{H^2+\breve{x}_n^2}}\end{bmatrix}^T. \tag{3}$$

Utilizing both $\breve{\mathbf{x}}_n$ and $\mathbf{y}_n$, the state variables at the nth time slot can be estimated by $\hat{\mathbf{x}}_n=\breve{\mathbf{x}}_n+\mathbf{K}_n(\mathbf{y}_n-\mathbf{h}(\breve{\mathbf{x}}_n))$ and the estimation MSE matrix at the nth time slot can be given by $\mathbf{M}_n=(\mathbf{H}_n^H\mathbf{Q}_{\mathrm{m},n}^{-1}\mathbf{H}_n+\mathbf{M}_{\mathrm{p},n}^{-1})^{-1}$.

The accuracy of the estimated state variables at the nth time slot can be characterized by the predicted PCRB. In particular, We assume that the process noise intensity is small so that $\mathbf{M}_n$ can be approximated by the predicted estimation MSE matrix $\breve{\mathbf{M}}_n=\mathbf{M}_n|_{\mathbf{x}_n=\breve{\mathbf{x}}_n}$ [11], [12]. As such, the predicted PCRB for the estimated relative position and velocity are given by $\mathrm{P\breve{C}RB}_{\mathrm{x},n}=[\breve{\mathbf{M}}_n]_{11}=F_{\mathrm{x}}(\breve{\mathbf{x}}_n)/D(\breve{\mathbf{x}}_n)$ and $\mathrm{P\breve{C}RB}_{\mathrm{v},n}=[\breve{\mathbf{M}}_n]_{22}=F_{\mathrm{v}}(\breve{\mathbf{x}}_n)/D(\breve{\mathbf{x}}_n)$, where $F_{\mathrm{x}}(\breve{\mathbf{x}}_n)$, $F_{\mathrm{v}}(\breve{\mathbf{x}}_n)$ and $D(\breve{\mathbf{x}}_n)$ are detailed in (4)-(5) at the top of the next page.

C. Problem Formulation

In this paper, we consider online UAV trajectory optimization for target tracking. At each time slot, the predicted state variables are optimized to minimize the weighted sum of predicted PCRBs. The optimization problem is formulated as

$$(\mathrm{P1.n}):\min_{\breve{\mathbf{x}}_n}\quad \alpha\mathrm{P\breve{C}RB}_{\mathrm{x},n}+(1-\alpha)\mathrm{P\breve{C}RB}_{\mathrm{v},n} \tag{7}$$

$$\text{s.t.}\ \sum_{n=1}^{N}E_n\le E_{\mathrm{tot}},\forall n\in\{1,2,...,N\}, \tag{7a}$$

$$|\eta_{n-1}-\breve{x}_n|\le v_{\mathrm{A,max}}\Delta T, \tag{7b}$$

$$\breve{x}_n-\Delta T\breve{v}_n-\hat{x}_{n-1}=0, \tag{7c}$$

$$x_{\mathrm{A},0}=x_{\mathrm{I}},\quad x_{\mathrm{A},N}=x_{\mathrm{F}}, \tag{7d}$$

where $\alpha\in[0,1]$ denotes the regularized weighting factor,[4] $E_n=P(v_{\mathrm{A},n})\Delta T$ denotes the UAV propulsion energy consumption at the nth time slot, E_{tot} denotes the total propulsion energy budget, the variable η_{n-1} is defined as $\eta_{n-1}\triangleq\hat{x}_{n-1}+\hat{v}_{n-1}\Delta T+v_{\mathrm{A},n-1}\Delta T$, $v_{\mathrm{A,max}}$ denotes the UAV maximum velocity and $x_{\mathrm{A},n}$ denotes the UAV position at the nth time slot. $P(v_{\mathrm{A},n})$ denotes the UAV propulsion power given by (6), where P_0, P_{i}, U_{tip}, v_{h} and χ are related constant parameters specified in [7]. In (P1.n), (7a) represents the total UAV propulsion energy consumption constraint during the whole flight. (7b), (7c) and (7d) represents the UAV maximum velocity constraint, the predicted state variables coupling constraint and the UAV initial-final location constraint, respectively. Note that optimizing the predicted state variables is equivalent to the UAV trajectory design due to (2) and $x_{\mathrm{A},n}=x_{\mathrm{A},n-1}+v_{\mathrm{A},n}\Delta T$.

(P1.n) is a non-convex optimization problem due to the non-convex objective function and the constraint (7a). Moreover, note that (P1.n) represents an online UAV trajectory optimization problem because, at the nth time slot, both the UAV trajectory and propulsion energy consumption at the following time slots have been undetermined. However, constraints (7a) and (7d) must be considered when optimizing the UAV trajectory for each time slot. Otherwise, the sequentially generated UAV trajectory may not be feasible for both constraints, such as the overuse of propulsion energy at the current time slot. Thus, it is non-trivial to solve (P1.n) while ensuring the feasibility of the obtained solution.

III. Proposed Approach

In this section, an online UAV trajectory optimization approach is proposed to solve (P1.n). Note that, at the nth time slot, the undetermined UAV trajectory can be divided into the trajectory to be optimized at the current time slot and the trajectory at future time slots, denoted by $x_{\mathrm{A},n}$ and $\{x_{\mathrm{A},l}\}, l=n+1,...,N$, respectively. If the undetermined UAV trajectory is specified, then the feasibility of the solution to (P1.n) can be judged at the nth time slot. As a result, the idea of our approach is to design $x_{\mathrm{A},n}$ and $\{x_{\mathrm{A},l}\}$ by solving two subproblems, named as the *candidate trajectory* and the *energy-aware backup trajectory* optimization problem, respectively. The subproblems and the procedures of our proposed approach are specified as follows.

1) Initialization: We first define a variable $E_{\mathrm{c},n}\triangleq\sum_{m=1}^{n-1}E_m$ as the consumed UAV propulsion energy until the $(n-1)$th time slot. Particularly, $E_{\mathrm{c},1}=0$ and $n=1$ is initialized at the first time slot.

2) Candidate trajectory optimization: At the nth time slot, the candidate trajectory optimization problem is formulated as

$$(\mathrm{P2.n}):\min_{\breve{\mathbf{x}}_n}\quad \alpha\mathrm{P\breve{C}RB}_{\mathrm{x},n}+(1-\alpha)\mathrm{P\breve{C}RB}_{\mathrm{v},n} \tag{8}$$

$$\text{s.t. (7b),(7c)},$$

$$|\breve{x}_n-\omega_n|\le(N-n)v_{\mathrm{A,max}}\Delta T, \tag{8a}$$

with $\omega_n=x_{\mathrm{A},n-1}+\eta_{n-1}-x_{\mathrm{F}}$. In (P2.n), the constraint (8a) is derived from $|x_{\mathrm{F}}-x_{\mathrm{A},n}|\le(N-n)v_{\mathrm{A,max}}\Delta T$, representing that given the UAV position at the nth time slot, the UAV can arrive at the final location with its maximum velocity within the following $N-n$ time slots. In this way, the solution to (P2.n) is sure to satisfy the constraint (7d) in (P1.n).

Our proposed algorithm to solve (P2.n) is as follows. (P2.n) is a non-convex fractional programming problem and can be addressed via Dinkelbach's transform [14]. Specifically, we first reformulate the numerator and denominator of the objective function of (P2.n) as $A(\breve{\mathbf{x}}_n)=D(\breve{\mathbf{x}}_n)(H^2+\breve{x}_n^2)^8$ and

[4]In practice, the weighting factor can be designed to balance the position and velocity estimation errors according to specific sensing requirements.

$$\underline{t} = \max\{\eta_{n-1} - v_{\mathrm{A,max}}\Delta T, \omega_n - (N-n)v_{\mathrm{A,max}}\Delta T\}, \bar{t} = \min\{\eta_{n-1} + v_{\mathrm{A,max}}\Delta T, \omega_n + (N-n)v_{\mathrm{A,max}}\Delta T\}, \quad (11)$$

$B(\breve{\mathbf{x}}_n) = (\alpha F_{\mathrm{x}}(\breve{\mathbf{x}}_n) + (1-\alpha)F_{\mathrm{v}}(\breve{\mathbf{x}}_n))(H^2 + \breve{x}_n^2)^8$, respectively. Then, (P2.n) can be formulated as

$$(\mathrm{P2.n}'): \min_{\breve{\mathbf{x}}_n} \quad C(\breve{\mathbf{x}}_n) \quad \text{s.t.} \quad (7\mathrm{b}),(7\mathrm{c}),(8\mathrm{a}),$$

where $C(\breve{\mathbf{x}}_n) \triangleq -A(\breve{\mathbf{x}}_n) + \zeta B(\breve{\mathbf{x}}_n)$, and the auxiliary variable ζ is updated by $\zeta_{k+1} = A(\breve{\mathbf{x}}_{n,k}^*)/B(\breve{\mathbf{x}}_{n,k}^*)$ with $\breve{\mathbf{x}}_{n,k}^*$ denoting the solution to (P2.n′) in the kth iteration.

(P2.n′) is a polynomial program, and its global optimal solution can be obtained via Lasserre hierarchy [15]. To be specific, we substitute $(\breve{x}_n - \hat{x}_{n-1})/\Delta T$ into $\breve{v}_n$ due to the constraint (7c). Then, a slack variable $\mathbf{t}$ is introduced and defined as $\mathbf{t} \triangleq [t_1, t_2, ..., t_{17}]^T$ with $t_q = \breve{x}_n^q, q = 1, 2, ..., 17$. Given $\mathbf{t}$, $C(\breve{\mathbf{x}}_n)$ can be reformulated as $C(\mathbf{t}) = \mathbf{c}^T\mathbf{t}$, where $\mathbf{c} = [c_1, c_2, ..., c_{17}]^T$ denotes the monomial coefficient with $c_{17} = 0$ since the maximum degree of $\breve{x}_n$ in $C(\breve{\mathbf{x}}_n)$ is 16. Afterward, we define two Hankel matrices as

$$\mathbf{L}(\mathbf{t}) \triangleq \begin{bmatrix} 1 & t_1 & ... & t_8 \\ t_1 & t_2 & ... & t_9 \\ ... & ... & ... & ... \\ t_8 & t_9 & ... & t_{16} \end{bmatrix}, \mathbf{M}(\mathbf{t}) \triangleq \begin{bmatrix} t_1 & t_2 & ... & t_9 \\ t_2 & t_3 & ... & t_{10} \\ ... & ... & ... & ... \\ t_9 & t_{10} & ... & t_{17} \end{bmatrix}, \quad (9)$$

respectively. As such, (P2.n′) can be reformulated as

$$(\mathrm{P2.n}''): \min_{\mathbf{t}} \quad \mathbf{c}^T\mathbf{t} \quad \text{s.t.} \quad \bar{t}\,\mathbf{L}(\mathbf{t}) \succeq \mathbf{M}(\mathbf{t}) \succeq \underline{t}\,\mathbf{L}(\mathbf{t}), \quad (10)$$

where the expressions of $\underline{t}$ and $\bar{t}$ are shown in (11). The constraint in (10) is due to $\underline{t} \le \breve{x}_n \le \bar{t}$ [15, Proposition 2.1], which is the equivalent incorporation of (7b) and (8a). (P2.n″) is a semidefinite program (SDP) that can be optimally solved by CVX tools.

By solving (P2.n), a candidate UAV trajectory denoted by $x_{\mathrm{A},n}^* = x_{\mathrm{A},n-1} + \eta_{n-1} - \breve{x}_n^*$ is obtained for minimizing the weighted sum-predicted PCRBs at the nth time slot without the total energy consumption constraint (7a), where $\breve{\mathbf{x}}_n^* = [\breve{x}_n^*, \breve{v}_n^*]^T$ denotes the solution to (P2.n). Whether this candidate UAV trajectory $x_{\mathrm{A},n}^*$ is feasible for (P1.n) will be addressed after solving the following optimization problem.

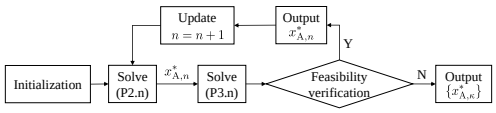

Fig. 2. The proposed approach procedures.

3) Energy-aware backup trajectory optimization: Given the solution to (P2.n), the energy-aware backup trajectory optimization problem can be formulated as

$$(\mathrm{P3.n}): \min_{\{v_{\mathrm{A},l}\}} \sum_{l=n+1}^{N} P(v_{\mathrm{A},l})\Delta T \quad (12)$$

$$\text{s.t.} \ |v_{\mathrm{A},l}| \le v_{\mathrm{A,max}}, \forall l, \quad (12\mathrm{a})$$

$$x_{\mathrm{A},l-1} = x_{\mathrm{A},n}^*, \quad x_{\mathrm{A},N} = x_{\mathrm{F}}. \quad (12\mathrm{b})$$

(P3.n) can be solved offline since it is irrelevant to the predicted PCRBs, which are calculated online following the EKF procedures. To address the non-convex objective function of (P3.n), slack variables denoted by $\{\xi_l\}$ are introduced such that $\xi_l \ge ((1 + v_{\mathrm{A},l}^4/(4v_{\mathrm{h}}^4))^{1/2} - v_{\mathrm{A},l}^2/(2v_{\mathrm{h}}^2))^{1/2} \ge 0$. As a result, the constraint $\xi_l^{-2} \le \xi_l^2 + v_{\mathrm{A},l}^2/v_{\mathrm{h}}^2$ should be satisfied. Note that $\xi_l^2 + v_{\mathrm{A},l}^2/v_{\mathrm{h}}^2$ is convex regarding to both ξ_l and $v_{\mathrm{A},l}$, and lower bounded by its first-order Taylor expansion at a given point $\{\xi_{l,r}, v_{\mathrm{A},l,r}\}$ in the rth iteration. Thus, we apply the SCA technique to approximate this constraint by

$$\xi_l^{-2} \le 2\xi_{l,r}(\xi_l - \xi_{l,r}) + \xi_{l,r}^2 + 2(v_{\mathrm{A},l} - v_{\mathrm{A},l,r})/v_{\mathrm{h}}^2 + v_{\mathrm{A},l,r}^2/v_{\mathrm{h}}^2. \quad (13)$$

Given (13), the solution to (P3.n) can be obtained by iteratively solving the following optimization problem formulated as

$$(\mathrm{P3.n}'): \min_{\{v_{\mathrm{A},l}\},\{\xi_l\}} \tilde{P} \quad (14)$$

$$\text{s.t.} \ \xi_l \ge 0, \forall l, \quad (14\mathrm{a})$$

$$(13),(12\mathrm{a}),(12\mathrm{b}),$$

with $\tilde{P} = \sum_{l=n+1}^{N} P_0(1 + 3v_{\mathrm{A},l}^2/U_{\mathrm{tip}}^2) + P_i\xi_l + \chi|v_{\mathrm{A},l}|^3/2$. (P3.n′) is a convex optimization problem and can be solved by CVX tools. Given the solutions to (P3.n) denoted by $\{v_{\mathrm{A},l}^*\}$, an energy-aware backup trajectory is obtained by $\{x_{\mathrm{A},l}^*\}$ with $\{x_{\mathrm{A},l}^*\}$ with $x_{\mathrm{A},l}^* = x_{\mathrm{A},l-1}^* + v_{\mathrm{A},l}^*\Delta T, l = n+1, ..., N$. The reason for such design is that it is easier for the candidate trajectory $x_{\mathrm{A},n}^*$ to be feasible if the UAV consumes as least propulsion energy as possible at the following time slots.

4) Feasibility verification and output: After solving (P2.n) and (P3.n), the feasibility of the candidate trajectory $x_{\mathrm{A},n}^*$ can now be verified. Specifically, let $E_{\mathrm{b},n} = \sum_{l=n+1}^{N} P(v_{\mathrm{A},l}^*)\Delta T$ denote the propulsion energy consumption for the energy-aware backup trajectory. If

$$E_{\mathrm{c},n} + P\left(\frac{x_{\mathrm{A},n}^* - x_{\mathrm{A},n-1}}{\Delta T}\right)\Delta T + E_{\mathrm{b},n} \le E_{\mathrm{tot}}, \quad (15)$$

holds, then the candidate trajectory $x_{\mathrm{A},n}^*$ satisfies the constraint (7a) and, therefore, can be output as the solution to (P1.n) with its feasibility guaranteed. Otherwise, the candidate trajectory is infeasible because it leads to the total propulsion energy consumption exceeding the budget E_{tot}. In this case, to ensure the feasibility of (P1.n), we resort to output the energy-aware backup trajectory obtained at the former time slot, i.e., $\{x_{\mathrm{A},\kappa}^*\}, \kappa = n, ..., N$ as the designed UAV trajectory at the rest time slots.[5] At the first time slot, if (15) is not satisfied, the UAV trajectory can be designed as the solution to (P3.n) with $n = 0$ and (12b) replaced by (7d). Note that the objective function in (14) is an upper bound of the objective function in (12) due to the slack operation. Thus, (15) is a sufficient condition for the optimized UAV trajectory to be feasible.

The aforementioned procedures are summarized in Fig.2. At each time slot, the UAV trajectory is optimized by solving (P2.n) for sensing performance maximization, and its feasibility of satisfying (7a) is verified by solving (P3.n) and further judging whether (15) holds. Note that $x_{\mathrm{A},n}^*$ is regardless of the propulsion energy consumption, while $\{x_{\mathrm{A},\kappa}^*\}$ minimizes the propulsion energy to be consumed. Therefore, our approach frees the UAV trajectory optimization from the total energy consumption constraint when there is enough energy left in real time, which offers excellent flexibility for sensing performance maximization.

The convergence of our proposed approach is analyzed as follows. Note that our proposed approach sequentially solves (P2.n) and (P3.n) unless (15) is not satisfied. Our proposed algorithm to solve (P2.n) is guaranteed to converge to the

[5]We assume (P2.n) and (P3.n) are feasible at the initial time slot.

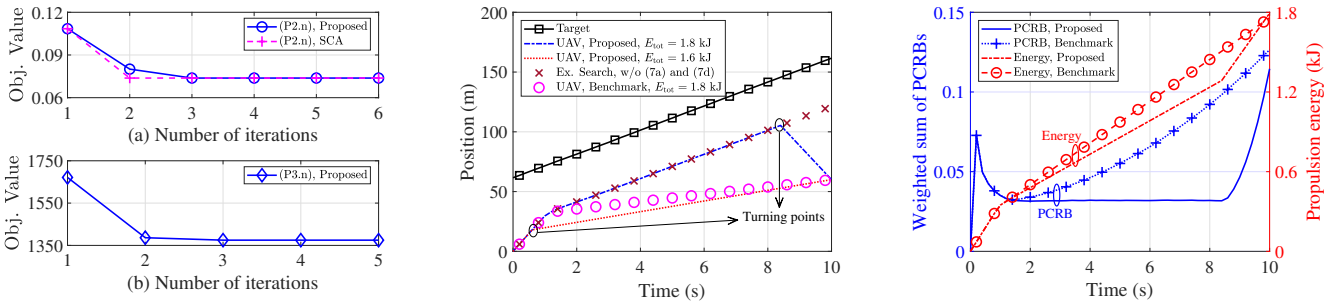

(a) Convergence behaviour. (b) UAV and target trajectories. (c) Energy consumption and sensing performance.

Fig. 3. Convergence behaviour of our proposed approach and performance comparisons with the benchmark.

global optimal solution. The reason is that if the reformulated problem (P2.n′) via Dinkelbach's transform can be optimally solved, then its solution converges to the optimal solution to (P2.n) [14]. Fortunately, this condition is satisfied because the Lasserre hierarchy on the polynomial program converges to the global optimal solution to (P2.n′′) [15]. Meanwhile, our algorithm to solve (P3.n) converges to a stationary point. Moreover, the computational complexity of our proposed approach at each time slot can be given as follows. Due to the dimension of $\mathbf{t}$ as 17, the computational complexity for solving (P2.n′′) and (P3.n′) can be given by $\mathcal{O}(17^{3.5})$ and $\mathcal{O}((2(N-n))^{3.5})$, respectively [16]. Thus, the overall computational complexity of our proposed approach at the nth time slot can be given by $\mathcal{O}(17^{3.5}J_{\rm D} + (2(N-n))^{3.5}J_{\rm S})$, where $J_{\rm D}$ and $J_{\rm S}$ denote the number of iterations required for convergence of Dinkelbach's transform and SCA, respectively.

IV. Numerical Results

This section provides numerical results to illustrate the effectiveness of our proposed UAV trajectory optimization approach. Unless specified otherwise, the numerical values of key system parameters are set as follows: $P_0 = 79.8563$ W, $P_i = 88.6279$ W, $U_{\rm tip} = 120$ m/s, $v_{\rm h} = 4.03$ m/s, $\chi = 0.0185$ kg·m^2 [7], $P_{\rm A} = 20$ dBm, $N_{\rm sym} = 10^4$, $\Delta T = 0.2$ s, $\lambda = 0.01$ m, $\sigma^2 = -80$ dBm, $\tilde{q} = 1$, $\varepsilon = 100$ m^2, $N_{\rm t} = N_{\rm r} = 16$, $a_1 = 0.1$, $a_2 = 10$, $a_3 = 2000$, $\alpha = 0.5$, $\phi_0 = 40°$, the target average velocity $v_{{\rm T},0} = 10$ m/s and $H = 50$ m [12]. Our proposed approach is compared with a benchmark: at the nth time slot, if there is enough propulsion energy for direct flight to the final location at the following time slots, represented by $E_{\rm tot} - E_{{\rm c},n} > P(v_{\rm A,max})\Delta T + (N-n)P(v_{{\rm df},n})\Delta T$ with $v_{{\rm df},n} = (x_{\rm F} - x_{{\rm A},n})/(N-n)\Delta T$, then the UAV trajectory is obtained by solving (P1.n) with the constraint (7a) replaced with $E_n \le E_{\rm tot} - E_{{\rm c},n}$. Otherwise, the remaining UAV velocity is designed as $v_{{\rm df},n-1}$.

Fig.3(a) demonstrates the convergence behaviour of our proposed approach at a typical time slot $n = 1$, in the case with $x_{\rm I} = 0$ m, $x_{\rm F} = 60$ m and $E_{\rm tot} = 1.6$ kJ. The abbreviation "obj. value" refers to the objective function value. It can be observed that our proposed approach converges after about 4 iterations. Compared to the existing SCA algorithm [10], [11], our proposed algorithm to solve (P2.n) converges slower but has approximately the same number of iterations for convergence, i.e., $J_{\rm D} \approx J_{\rm S}$. This makes the computational complexity of our proposed algorithm higher than that of the SCA given by $\mathcal{O}(J_{\rm S})$ [10], [11] due to the additional dimension of $\mathbf{t}$. In addition, the computational complexity of our algorithm to solve (P3.n) is equivalent to that of the SCA-based subalgorithm in [8]. However, the superiority of our proposed algorithm to solve (P2.n) lies in its global optimality compared to the existing SCA algorithm [10], [11]. For example, in the case with $\phi_0 = 89°$ and $v_{{\rm T},0} = 2$ m/s, we set a random initial point as uniformly distributed in the feasible region and run 10^4 times Monte Carlo simulations to obtain the statistic (stat.) frequency of solutions to (P2.n) reached by the exhaustive (ex.) search, our proposed approach and SCA. The results are given in Table I, which shows that our proposed algorithm reaches the optimal solution with a 100% statistic frequency. In comparison, SCA potentially achieves a suboptimal solution, which results in 153% worse sensing performance. Such results demonstrate the importance of solving (P2.n) optimally.

TABLE I
Optimality of our proposed and the existing approach.

Approach	Converged obj. value	Stat. frequency
Ex. search	0.1871	100%
Proposed	0.1871	100%
SCA	0.1871	66.7%
	0.4747	33.3%

In Fig.3(b), we show the target and UAV trajectories under the benchmark and our proposed optimization approach in one trial, with $x_{\rm I} = 0$ m, $x_{\rm F} = 60$ m, and the results picked every 0.6 s. As shown in Fig.3(b), in both cases with $E_{\rm tot} = 1.8$ kJ and $E_{\rm tot} = 1.6$ kJ, the indicated turning points appear because the condition (15) is no longer satisfied at that time slot. In other words, the UAV trajectory is transformed from the candidate trajectory minimizing the weighted sum of PCRBs into the energy-aware backup trajectory, since the UAV has to reach the final location given the limited remaining propulsion energy. The two turning points differ because 1.6 kJ is insufficient for the UAV to travel as far as the case with $E_{\rm tot} = 1.8$ kJ. Instead, the UAV resorts to flying towards the final location earlier with a certain velocity, which ensures that the total propulsion energy budget is not exceeded. Particularly, the UAV trajectory ahead of the turning point matches the results obtained by solving (P1.n) via the exhaustive search method without the constraints (7a) and (7d), which verifies the effectiveness of the proposed algorithm to (P2.n). Moreover, compared to the benchmark, our proposed approach allows a much longer duration for the UAV trajectory to be optimized for maximizing the sensing performance under the case with $E_{\rm tot} = 1.8$ kJ, rendering it superior to the benchmark.

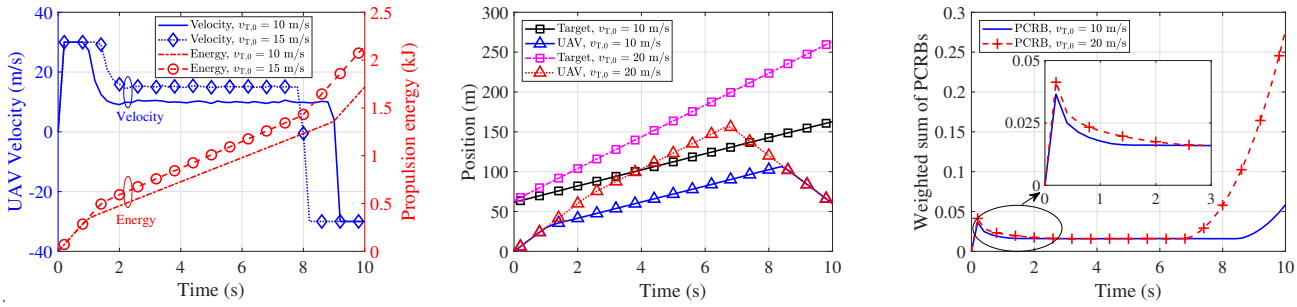

(a) Energy consumption. (b) UAV trajectories. (c) Sensing performance.

Fig. 4. Comparisons between the consumed propulsion energy, UAV trajectories and sensing performance under different target average velocities.

Fig.3(c) illustrates the propulsion energy consumption and the weighted sum of actual PCRBs achieved by the benchmark and our proposed approach under the cases with $E_{\mathrm{tot}} = 1.8$ kJ shown in Fig.3(a). The actual PCRBs are obtained by the diagonal elements of the estimation MSE matrix at the nth time slot $\mathbf{M}_n$. It is found that the total propulsion energy consumption under our proposed approach is smaller than 1.8 kJ, which validates the effectiveness of the solution to (P3.n) and the whole proposed UAV trajectory optimization approach. Additionally, compared to the benchmark, our proposed approach leads to less energy consumption ahead of the UAV turning points while utilizing more energy in total given the same energy budget E_{tot}. Besides, our proposed approach leads to a significantly lower weighted sum of actual PCRBs than the benchmark. These results show that our proposed approach achieves a substantial sensing performance improvement and a more flexible and sufficient utilization of propulsion energy than the benchmark.

In Fig.4(a), the propulsion energy consumption and the UAV velocity are compared when the target average velocity is set as 10 m/s and 15 m/s, respectively. It is demonstrated that in both cases, the UAV flies at its maximum velocity either when approaching the target at the beginning or when flying towards the final location at the final part of the flight. However, the UAV velocity remains approximately the same as the target average velocity for the rest of the flight. Furthermore, the propulsion energy is consumed slower when tracking the target in the case with $v_{\mathrm{T},0} = 10$ m/s because the UAV velocity is closer than 15 m/s to the maximum-endurance velocity, which is approximately 10.21 m/s [7]. This phenomenon shows that, apart from the initial-final location constraint, the target velocity fundamentally affects the UAV energy consumption. Fig.4(b) and Fig.4(c) illustrate the UAV trajectories and sensing performance in two cases with $v_{\mathrm{T},0} = 10$ m/s and $v_{\mathrm{T},0} = 20$ m/s, respectively. The total UAV propulsion energy budget is $E_{\mathrm{tot}} = 2$ kJ. In both cases, a constant minimal weighted sum of PCRBs is achieved when the UAV keeps relatively static with respect to the target. Otherwise, the target velocity affects the duration of the UAV approaching or leaving the target, during which the weighted sum of PCRBs is higher than the minimal value.

V. Conclusion

In this work, a novel online UAV trajectory optimization approach was proposed for ensuring the feasibility of satisfying both the total propulsion energy constraint and the initial-final location constraint. Our approach achieves this goal by solving two subproblems for sensing performance maximization and propulsion energy consumption minimization, respectively. Then, we proposed algorithms that optimally solve the sensing performance maximization problem and efficiently solve the propulsion energy consumption minimization problem. Simulation results verified our proposed approach's effectiveness, further illustrating its pronounced superiority to benchmarks. Applying our proposed approach in multi-UAV collaborated sensing scenarios is worthwhile for future studies.

References

[1] K. Meng *et al.*, "UAV-enabled integrated sensing and communication: Opportunities and challenges," *IEEE Wireless Commun.*, vol. 31, no. 2, pp. 97–104, Apr. 2024.

[2] Z. Fei, X. Wang, N. Wu, J. Huang, and J. A. Zhang, "Air-ground integrated sensing and communications: Opportunities and challenges," *IEEE Commun. Mag.*, vol. 61, no. 5, pp. 55–61, May 2023.

[3] Q. Wu *et al.*, "A comprehensive overview on 5G-and-beyond networks with UAVs: From communications to sensing and intelligence," *IEEE J. Sel. Areas Commun.*, vol. 39, no. 10, pp. 2912–2945, Oct. 2021.

[4] Y. Zeng, R. Zhang, and T. J. Lim, "Throughput maximization for UAV-enabled mobile relaying systems," *IEEE Trans. Commun.*, vol. 64, no. 12, pp. 4983–4996, Dec. 2016.

[5] Q. Wu, Y. Zeng, and R. Zhang, "Joint trajectory and communication design for multi-UAV enabled wireless networks," *IEEE Trans. Wireless Commun.*, vol. 17, no. 3, pp. 2109–2121, Mar. 2018.

[6] Y. Zeng and R. Zhang, "Energy-efficient UAV communication with trajectory optimization," *IEEE Trans. Commun.*, vol. 16, no. 6, pp. 3747–3760, Jun. 2017.

[7] Y. Zeng, J. Xu, and R. Zhang, "Energy minimization for wireless communication with rotary-wing UAV," *IEEE Trans. Wireless Commun.*, vol. 18, no. 4, pp. 2329–2345, Apr. 2019.

[8] S. Hu, X. Yuan, W. Ni, and X. Wang, "Trajectory planning of cellular-connected UAV for communication-assisted radar sensing," *IEEE Trans. Commun.*, vol. 70, no. 9, pp. 6385–6396, Sep. 2022.

[9] A. Khalili *et al.*, "Efficient UAV hovering, resource allocation, and trajectory design for ISAC with limited backhaul capacity," *IEEE Trans. Wireless Commun.*, vol. 23, no. 11, pp. 17 635–17 650, Nov. 2024.

[10] X. Jing, F. Liu, C. Masouros, and Y. Zeng, "ISAC from the sky: UAV trajectory design for joint communication and target localization," *IEEE Trans. Wireless Commun.*, vol. 23, no. 10, pp. 12 857–12 872, Oct. 2024.

[11] J. Wu, W. Yuan, and L. Bai, "On the interplay between sensing and communications for UAV trajectory design," *IEEE Internet Things J.*, vol. 10, no. 23, pp. 20 383–20 395, Dec. 2023.

[12] Y. Jiang, Q. Wu, W. Chen, and K. Meng, "UAV-enabled integrated sensing and communication: Tracking design and optimization," *IEEE Commun. Lett.*, vol. 28, no. 5, pp. 1024–1028, May 2024.

[13] Y. Bar-Shalom, X. R. Li, and T. Kirubarajan, *Estimation with Applications to Tracking and Navigation*, New York, USA: Wiley, 2001.

[14] W. Dinkelbach, "On nonlinear fractional programming," *Manage. Sci.*, vol. 13, no. 7, pp. 492–498, Mar. 1967.

[15] J. B. Lasserre, "Semidefinite programming vs. LP relaxations for polynomial programming," *Math. Oper. Res.*, vol. 27, no. 2, pp. 347–360, May 2002.

[16] Y. Zhao, Q. Wu, G. Chen, W. Chen, R. Liu, M.-M. Zhao, Y. Wu, and S. Ma, "Intelligent reflecting surface aided multi-tier hybrid computing," *IEEE J. Sel. Top. Signal Process.*, vol. 18, no. 1, pp. 83–97, Jan. 2024.